

6. Interpretation of results

6.1. The magnitude of the two resistances (diffusion and integration steps)

The overall crystal growth phenomenon can be considered as the combination of 3 steps, namely volume diffusion, surface reaction, and heat transfer. The first step is the mass transport of the growth units by diffusion or convection from the bulk of the solution to the crystal surface. The second step is the integration of units into the crystal lattice. The third step are heat related effects from the liberation of the crystallization heat when the crystal grow, and from the heat transfer connected with the mass transfer from and to the phase boundary (liquid/solid) [1–3]. Here the effect of heat transfer can be neglected due to the fact that the value of $\beta_d < 10^{-2}$ [3], and the value of $-\Delta H/(1-w_b)$ is less than 700 J g^{-1} [113]. Therefore, the crystal growth processes from solutions are dominantly either diffusion or reaction controlled. A change in the dominating growth mechanism arises by a change of temperature level or e.g. by traces of certain impurities or additives.

6.1.1. NaCl experiments

As mentioned before, see the theory (**Chapter 3.1.**), the dissolution process for pure and impure solutions is running faster than the growth process. Therefore, a possible surface disintegration resistance is here difficult to observe [4, 5]. The diffusion rate constant, k_d , was, therefore, estimated from the experimental dissolution rate by curve fitting of Eq. 3.11. The integration order, r , and the integration rate constant, k_r , were estimated from Eq. 3.10 by curve fitting of the growth rate data. k_r , k_d and r values for pure and impure solution are presented in **Table 6.1.1.**

In order to quantify the resistance in growth offered by the volume diffusion or surface reaction the effectiveness factors for surface integration and diffusion was used. When D_a is large, growth is diffusion controlled and the integration effectiveness factor η_r approaches $1/D_a$. Conversely, when D_a is small η_r approaches one, the growth is therefore controlled by the integration step. η_d and η_r values for NaCl crystal growth in pure and impure solution are given in **Table 6.1.1.** and shown in **Figs. 6.1.1.** and **6.1.2.** The effectiveness factor indicates that the controlling growth mechanism for NaCl

crystal growth in the pure NaCl solution is split into the diffusion step and the integration step. In the presence of impurities the obtained results indicate that the integration step offers a greater resistance to overall crystal growth rate than the diffusion step (see *Figs. 6.1.1.* and *6.1.2.* and *Table 6.1.1.*). The value of integration effectiveness factor, η_r , was approached one, this indicates that the crystal growth rate is controlled mainly by the integration step.

Table 6.1.1.: The kinetic parameters, η_d and η_r for NaCl crystal growth in the presence of different additives and the contribution in percent of growth resistance for the diffusion step and the integration step.

| Solution | r | k_r E-5 | k_d E-5 | η_r | η_d | Integ. % | Diffu. % |
|---|------|--------------|--------------|----------|----------|-------------|-------------|
| NaCl | 1.12 | 7.75 | 4.84 | 0.37 | 0.52 | 0.42 | 0.58 |
| NaCl-MgCl_2 | 1.33 | 1.56 | 6.28 | 0.80 | 0.16 | 0.83 | 0.17 |
| NaCl-PbCl_2 | 1.04 | 0.47 | 12.7 | 0.96 | 0.04 | 0.96 | 0.04 |
| $\text{NaCl-K}_2\text{Fe}(\text{CN})_6$ | 0.42 | 0.26 | 2.67 | 0.98 | 0.06 | 0.94 | 0.06 |

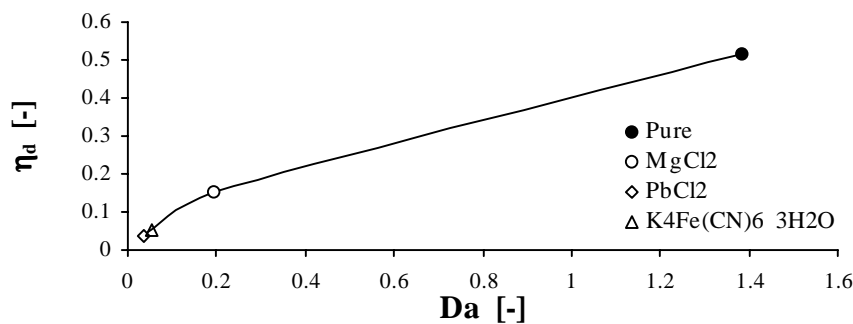


Figure 6.1.1.: Diffusion effectiveness factor for crystal growth rate of NaCl at different additives.

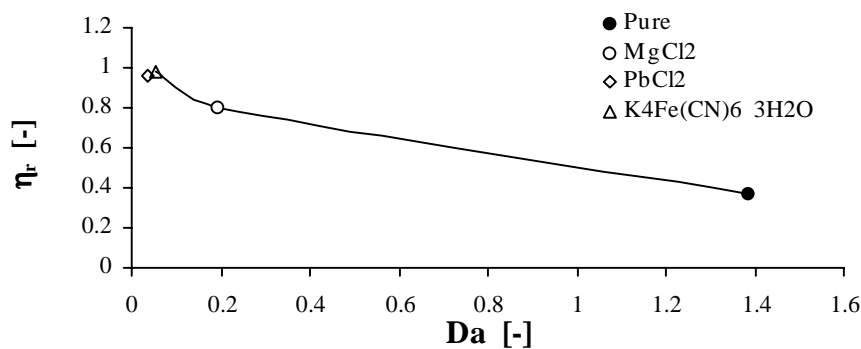


Figure 6.1.2.: Integration effectiveness factor for crystal growth rate of NaCl at different additives.

6.1.2. $MgSO_4 \cdot 7H_2O$ experiments

As mentioned previously the concept of the effectiveness factors for the volume diffusion and surface integration are used to qualify the resistance to either growth dominated by the diffusion or integration controlled. The integration order r and the integration rate constant k_r were estimated from Eq. 3.10, by curve fitting of the growth rate data. k_r , k_d and r values for pure and impure solution are presented in **Table 6.1.2.**

Table 6.1.2.: The kinetic parameters, η_d and η_r for $MgSO_4 \cdot 7H_2O$ crystal growth in the presence of different additives and the contribution in percent of growth resistance for the diffusion step and the integration step.

| <i>Solution</i> | <i>r</i> | <i>k_r</i> E-5 | <i>k_d</i> E-5 | η_r | η_d | <i>Integ.</i> % | <i>Diffu.</i> % |
|-----------------------------------|----------|-----------------------------|-----------------------------|----------|----------|--------------------|--------------------|
| $MgSO_4 \cdot 7H_2O$ | 0.96 | 7.6 | 3.05 | 0.30 | 0.72 | 0.29 | 0.71 |
| $MgSO_4 \cdot 7H_2O$ –Borax | 1.24 | 2.29 | 1.09 | 0.33 | 0.59 | 0.36 | 0.64 |
| $MgSO_4 \cdot 7H_2O$ – $FeSO_4$ | 1.72 | 1.7 | 1.98 | 0.42 | 0.40 | 0.51 | 0.49 |
| $MgSO_4 \cdot 7H_2O$ – K_2SO_4 | 0.98 | 3.72 | 1.85 | 0.41 | 0.60 | 0.41 | 0.59 |
| $MgSO_4 \cdot 7H_2O$ –KCl | 1.39 | 1.81 | 3.26 | 0.53 | 0.37 | 0.59 | 0.41 |
| $MgSO_4 \cdot 7H_2O$ – KH_2PO_4 | 0.93 | 3.47 | 1.94 | 0.45 | 0.57 | 0.44 | 0.56 |
| $MgSO_4 \cdot 7H_2O$ – Na_2SO_4 | 1.1 | 2.08 | 2.12 | 0.55 | 0.42 | 0.57 | 0.43 |
| $MgSO_4 \cdot 7H_2O$ – $NiSO_4$ | 1.22 | 2.97 | 2.09 | 0.43 | 0.50 | 0.46 | 0.54 |

Figs. 6.1.3. and **6.1.4.** show the diffusion and integration effectiveness factors for $MgSO_4 \cdot 7H_2O$ crystals, respectively. Growth in pure and impure solution were estimated for different supersaturation levels. The effectiveness factor results indicate that the controlling growth mechanism is contributing by means of the diffusion and the integration steps on the crystal growth of $MgSO_4 \cdot 7H_2O$ from pure and impure solution. It is clear from the obtained results that, the diffusion step offers a greater resistance to overall crystal growth rate than the integration step in the case of pure solution. While in the presence of different impurities, the dominating growth

mechanism changes and the integration step offers a greater resistance to overall crystal growth rate than the diffusion step (e.g. $FeSO_4$, KCl and Na_2SO_4 , see **Table 6.1.6**).

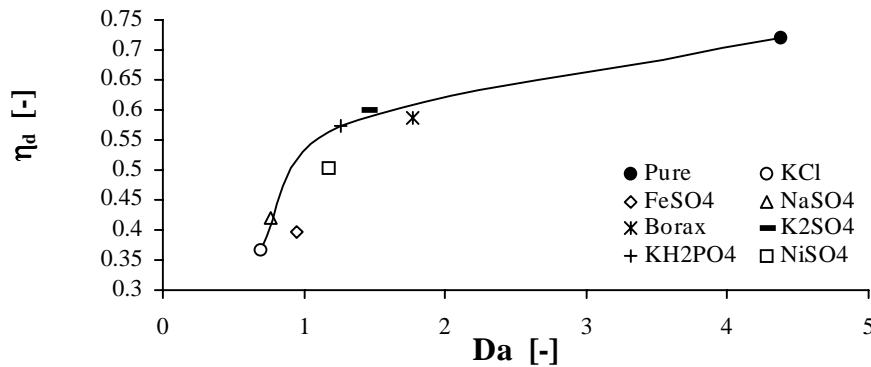


Figure 6.1.3.: Diffusion effectiveness factor for crystal growth rate of $MgSO_4 \cdot 7H_2O$ at different additives.

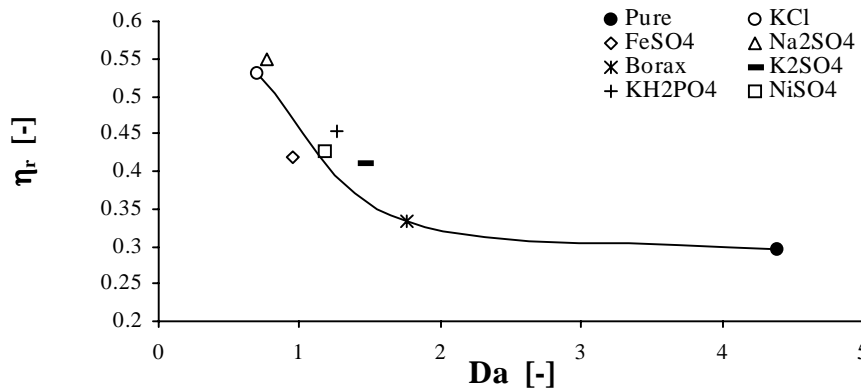


Figure 6.1.4.: Integration effectiveness factor for crystal growth rate of $MgSO_4 \cdot 7H_2O$ at different additives.

There are some differences between own conclusion [85] in case of $NaCl$ crystal growth from pure solution and the conclusions of Zhang et al. [83]. They concluded, that in the case of linear growth and dissolution rates and an equal slope for the crystal growth the growth can be called “diffusion controlled”. With the above assumptions it has been shown that $NaCl$ is diffusion controlled growing in the absence of impurities. However, with the used impurities a change in the dominating growth mechanism arises, i.e. the presence of certain impurities lead to a more important role of the reaction step. *In this work it is proven by means of the effectiveness factor concept, that there is almost a match of the integration step and the diffusion step for $NaCl$ crystal growth from pure solution, which is contrary to literature (e.g. [83]).*

6.2. Kinetic effect

Surface adsorbed impurities can reduce the measured growth rate of crystals by reducing or hindering the movement of growth steps on the crystal surfaces. Depending on the amount and strength of adsorption the effect on crystal growth can be very strong or hardly noticeable. Two extremes cases, i.e. adsorption at kinks (mobile impurities) and the surface terrace (immobile impurities), may be distinguished. The models of impurity adsorption considering kinks and the surface terraces deal with the kinetic aspect of adsorption of impurities of F faces, neglecting the thermodynamic effects.

6.2.1. NaCl experiments

The Eq. 3.39 enables to calculate K from the experimental $R_G(c_{imp})$ data. The best fits of Eq. 3.39 to the experimental data with a least-squares method are shown in **Fig. 6.2.1.** The fitted results are shown in **Fig. 6.2.1.** with solid lines for $PbCl_2$ as impurity. It is clear that the relative mass growth rate of $NaCl$ is reduced to zero. Therefore, this result may be considered to be examples of the case of $\alpha \cong 1$ (see [49]). Here, the concentration of impurity on the crystal surface is assumed to be in equilibrium with the concentration of the impurity in the solution, i.e. the distance between impurity on the surface is approximately the same as the critical diameter $2\rho_c$ at $\theta=1$, i.e. a full coverage of the crystal surface leads to growth rates equal to zero.

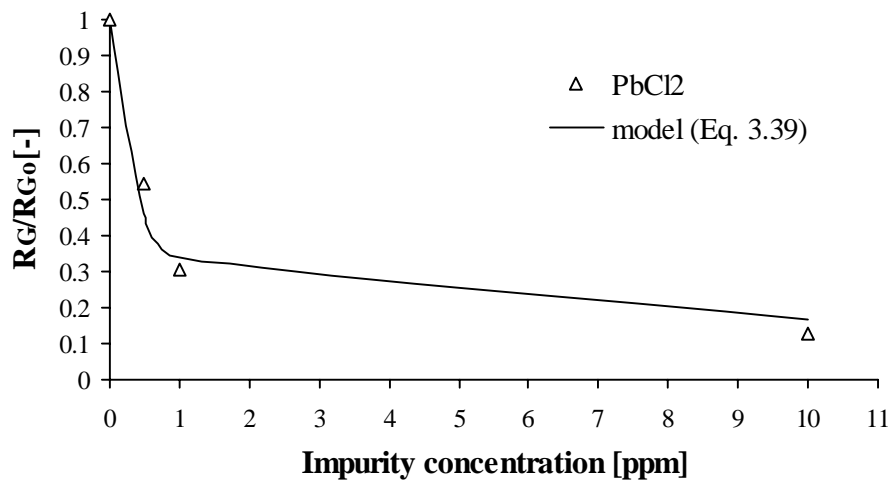


Figure 6.2.1.: Effect of $PbCl_2$ impurity on the relative mass growth rate of $NaCl$. Comparison of own work [114] with the model [Eq. 3.39].

While in the presence of $MgCl_2$ the relative mass growth rate of $NaCl$ is reduced and approaching a non-zero value. The parameter α is determined by fitting of Eq. 3.39 as shown in **Table 6.2.1.** According to the Kubota-Mullin model [49] this may be considered to be an example of the case $\alpha < 1$. In the case of $\alpha < 1$, the distance between impurity on the surface is larger than the critical radius of the two-dimensional nucleus $2\rho_c$, even at $\theta = 1$. Hence, the step can easily squeeze out between the impurity, i.e. the impurity is more easily adsorbed on crystal faces, but it has a weaker suppression effect.

Fig. 6.2.2. illustrates the plot of the impurity effect, $\alpha\theta_{eq}$, of adsorption-active sites as a function of Pb^{+2} impurity concentration. Experimental adsorption data are in good agreement with the theoretical Langmuir adsorption isotherm, which was drawn using the value of K determined above from crystal growth experiments. This agreement supports the validity of the Kubota-Mullin model [49].

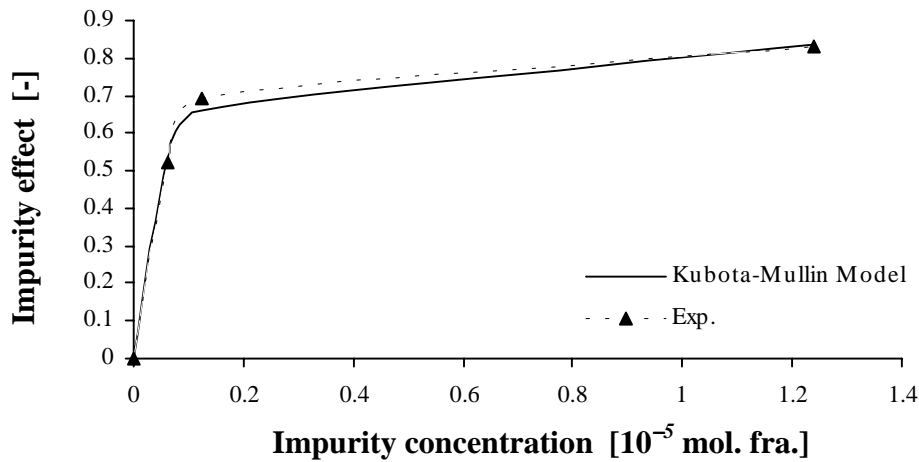


Figure 6.2.2.: Experimental isotherm of Pb^{+2} impurity adsorption onto $NaCl$ crystals
Comparison of own work [114] with the model [Eq. 3.39].

It can be seen from analysis of growth kinetics data that the $R_G(c_{imp})$ data follow a kink and terrace adsorption mechanism with a Langmuir adsorption isotherm. The value of heat adsorption is higher during adsorption at kinks than those involved in adsorption at the surface terraces [14]. Therefore, from the values of the heat adsorption as shown in **Fig. 6.2.2.**, it may be concluded that adsorption of the impurity Mg^{+2} occurs at kinks.

The relatively low values of the heat of adsorption indicates that adsorption is physical in nature. From **Fig. 6.2.3.** it is interesting to note that when the value of supersaturation increases the value of the heat of adsorption Q_{diff} has the tendency to

increase while the average distance, λ , between adsorption sites decreases (see **Table 6.2.1.**). The former argument is associated with an increasing competition of solute ions in occupying the same sites with the impurity ions. The later reasoning on the other hand is a consequence of a decrease in the average distance between kinks with increasing supersaturation.

Table 6.2.1.: Adsorption parameters for the growth of NaCl crystal at different supersaturations and impurities.

| <i>Solution</i> | σ % | <i>Adsorption mechanism</i> | α | K (mol/mol) ⁻¹ | λ (m) | l (m) | Q_{diff} (kJ/mol) |
|------------------------------|---------------|-----------------------------|----------|--------------------------------|------------------|------------------|------------------------|
| <i>NaCl–MgCl₂</i> | 0.18 | Kink | 0.55 | 2.70E+04 | 145 _a | 162 _a | 25.7 |
| | | Terrace | 0.6 | 7.40E+03 | 132 _a | 190 _a | 22.4 |
| | 0.36 | Kink | 0.57 | 5.20E+04 | 69 _a | 73 _a | 27.4 |
| | | Terrace | 0.57 | 2.30E+04 | 69 _a | 78 _a | 25.3 |
| <i>NaCl–PbCl₂</i> | 0.09 | Kink | 0.92 | 1.90E+06 | 175 _a | 183 _a | 36.4 |
| | | Terrace | 0.92 | 8.00E+05 | 175 _a | 193 _a | 34.2 |
| | 0.27 | Kink | 0.91 | 1.90E+06 | 57 _a | 60 _a | 36.4 |
| | | Terrace | 0.91 | 8.10E+05 | 57 _a | 63 _a | 34.3 |
| | 0.36 | Kink | 0.86 | 2.70E+06 | 45 _a | 46 _a | 37.3 |
| | | Terrace | 0.9 | 2.30E+05 | 43 _a | 58 _a | 31.1 |

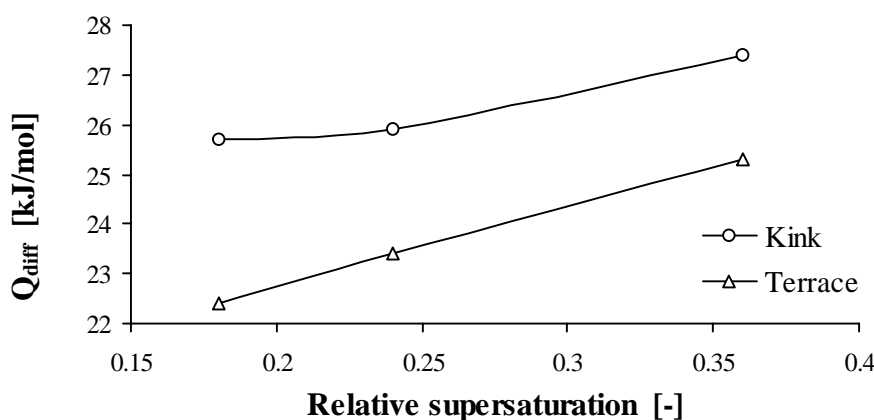


Figure 6.2.3.: The differential heat of adsorption at different supersaturation. Adsorption of Mg^{+2} ions on crystal surface of NaCl.

Table 6.2.1. shows the impurity effectiveness factor, α , that is determined from the growth experiments as a function of the reciprocal of the relative supersaturation $1/\sigma$. As expected from Eq. 3.33 α increases linearly with a slope equal to $\gamma a/k_B T \lambda$. Therefore, if the value of the edge free energy, γ , is known at a given temperature, T , the average distance, λ , between the adsorption-active sites can be estimated from the Kubota-Mullin model [49] as a function of the growth unit, a . According to Hayashi and Schichiri [115] for *NaCl* crystals growing in aqueous solution the edge free energy, γ , per growth unit is 6.0×10^{-22} J/m. Therefore, $\gamma/k_B T = 0.14$ at $T = 303.15$ (30°C) the temperature of growth rate measurements in this study. However, α is known by fitting of Eq. 6, $\alpha = (\gamma/k_B T)(a/\lambda)$. These two values give the average distance, λ , between the adsorption-active sites as shown in *Table 6.2.1.* The spacing, l , between the neighbouring active sites occupied by impurities can also be estimated from the relation $\theta_{eq} = \lambda/l$ if the impurity concentration is known. It is clear from *Table 6.2.1.* that these estimated values of λ and l seem to be reasonable, although direct experimental verification is impossible.

6.2.2. *MgSO₄•7H₂O* experiments

For a validation of the experimentally found data a comparison with the Kubota-Mullin model [49] was carried out. As shown in *Fig. 6.2.4.*, the relative growth rate of *MgSO₄•7H₂O* is reduced asymptotically to zero. Values of the parameter α were determined by fitting Eq. 3.39 to own data. The fitted results are shown in *Fig. 6.2.4.* with solid lines for Borax as impurity. The values of α , for different impurities, are given in *Table 6.2.2.* Therefore, some of these results may be considered to be examples of the case of $\alpha \cong 1$. Here, the concentration of the impurity on the surface of the crystal is assumed to be in equilibrium with the concentration of the impurity in the solution, i.e. the distance between impurity on the surface approximately the same as the critical diameter $2\rho_c$ at $\theta = 1$, i.e. a full coverage of the crystal surface leads to growth rates equal to zero.

In the presence of *K₂SO₄*, $\alpha \cong 0.5$, the relative mass growth rate of *MgSO₄•7H₂O* is reduced and approaching a non-zero value. According to the Kubota-Mullin model [49] this is may be considered to be an example of the case $\alpha < 1$. In the

case of $\alpha < 1$, as mentioned previously, the step can easily squeeze out between the impurity, i.e. the impurity is more easily adsorbed on crystal faces, but it has a weaker suppression effect.

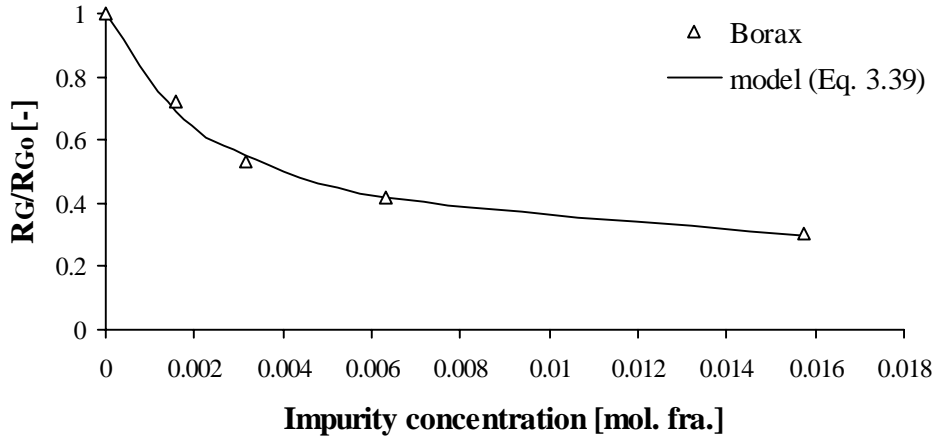


Figure 6.2.4.: Effect of Borax on the relative growth rate of $MgSO_4 \cdot 7H_2O$. Comparison of own work [107] with the model (Eq. 3.39).

It can also be seen from **Table 6.2.2.** that the $R_G(c_{imp})$ data follow kink and terrace adsorption mechanisms according to Langmuir adsorption isotherm. The values of heat adsorption are higher during adsorption at kinks than those involved in adsorption at the surface terraces [14]. Therefore, from the values of the heat adsorption given in **Table 6.2.2.** and **Fig. 6.2.5.**, in this figure the borax is taken as example, it may be concluded that at low supersaturated solution adsorption of impurities occurs at kinks. By increasing the supersaturation, the adsorption of impurities at kinks approximately approaches a constant value.

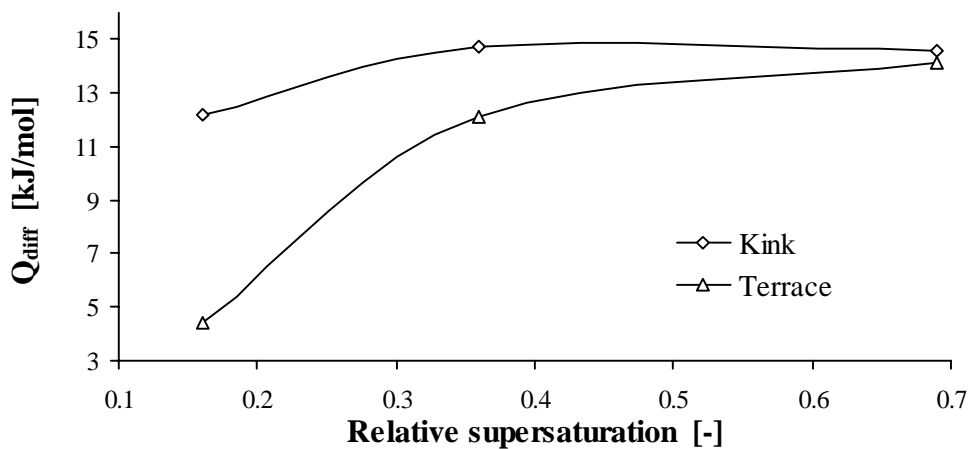


Figure 6.2.5.: The differential heat of adsorption, (Q_{diff}), at different supersaturation.

Table 6.2.2.: Adsorption parameters for the growth of $MgSO_4 \cdot 7H_2O$ crystals in the presence of Borax as impurity at different supersaturations.

| <i>Impurities</i> | σ % | <i>Adsorption Mechanism</i> | α | K (mol/mol) ⁻¹ | λ | Q_{diff} (kJ/mol) |
|-------------------------------------|---------------|---------------------------------|----------|--------------------------------|-----------|------------------------|
| <i>Borax [106]</i> | 0.16 | Kink | 0.76 | 138 | 801a | 12.2 |
| | | Terrace | 0.8 | 5.9 | 338a | 4.4 |
| | 0.36 | Kink | 0.67 | 383 | 419a | 14.7 |
| | | Terrace | 0.69 | 131 | 406a | 12.1 |
| | 0.69 | Kink | 0.83 | 369 | 175a | 14.6 |
| | | Terrace | 0.73 | 300 | 199a | 14.1 |
| <i>FeSO₄</i> | 0.69 | Kink | 1.3 | 46 | 112a | 9.5 |
| | | Terrace | 2.5 | 3.3 | 58a | 3 |
| | 1.04 | Kink | 1.3 | 42 | 74a | 9.3 |
| | | Terrace | 2.2 | 4.1 | 44a | 3.5 |
| | 1.37 | Kink | 0.91 | 88 | 80a | 11 |
| | | Terrace | 1.16 | 15.7 | 63a | 6.8 |
| <i>K₂SO₄</i> | 0.36 | Kink | 0.58 | 60.2 | 483a | 10.2 |
| | | Terrace | 0.9 | 6.70 | 312a | 4.7 |
| | 0.69 | Kink | 0.5 | 137 | 292a | 12.2 |
| | | Terrace | 0.54 | 40 | 270a | 9.14 |
| | 1.04 | Kink | 0.49 | 67 | 196a | 10.4 |
| | | Terrace | 0.66 | 10.8 | 145a | 5.9 |
| <i>Na₂SO₄</i> | 0.69 | Kink | 0.91 | 32.3 | 160a | 8.6 |
| | | Terrace | 2.3 | 1.27 | 63a | 0.6 |
| | 1.04 | Kink | 1.14 | 21.3 | 84a | 7.6 |
| | | Terrace | 2.4 | 1.19 | 40a | 0.43 |
| | 1.72 | Kink | 0.91 | 32.3 | 64a | 8.6 |
| | | Terrace | 2.3 | 1.27 | 25a | 0.6 |
| <i>NiSO₄</i> | 0.69 | Kink | 1.09 | 53.7 | 134a | 9.9 |
| | | Terrace | 3.7 | 1.17 | 39a | 0.4 |
| | 1.04 | Kink | 1.06 | 45 | 90a | 9.4 |
| | | Terrace | 3.1 | 1.40 | 31a | 0.8 |
| | 1.37 | Kink | 0.95 | 52 | 77a | 9.8 |
| | | Terrace | 1.7 | 4.40 | 43a | 3.7 |

*The same argument that the values of the heat of adsorption at kinks are higher than the adsorption at surface terraces can be applied for other impurities investigated in this study (see **Table 6.2.2.**).*

Several papers dealing with the growth kinetics of crystals in the presence of impurities have been published [116], but there is no paper assessing the adsorption isotherm obtained from experiments through the kinetic model of crystal growth for a suspension growth condition as usual in industrial crystallization. For instance, recently Rauls et al. [117] reported the growth kinetics of ammonium sulfate crystals in the presence of the azo dyes amaranth and fuchsin. Adsorption isotherms were measured for these two impurities but no quantitative discussion was made regarding the growth suppressing caused by these impurities. *Hence, the present work is a successful attempt for assessing the adsorption isotherm from crystal growth experiments for a suspension growth condition.*

6.3. Thermodynamic effect

In the aqueous electrolyte solution two different species can be found, the dissociated ions (cations and anions) and the water molecules, there are different types of forces in the system: water-water, ion-ion, and water-ion interaction [118]. The simplest reaction of the metals, M^{n+} , in aqueous solutions is the loss of a proton to give the hydroxy species, $M(OH)^{(n-1)+}$. The coordination of metal ion to a water molecule will make a proton loss easier. The greater the positive charge on the metal ion, the easier it should be for proton to dissociate from an attached water molecule. Such an equilibrium is given the following equation [119]:



6.3.1. The effect of pH ($MgSO_4 \cdot 7H_2O$ experiments)

The dissociation of a proton from water molecules may effect the structure of the solution. By addition of Mg^{+2} ions to the water, the hydronium ions are generated as a result of the hydration of Mg^{+2} according to the equilibrium in Eq. 6.1 and as shown in the following expression:



The addition of hydronium ions (H_3O^+) to the solution will affect the position of the equilibrium. According to Le Chatelier principle the position of chemical equilibrium always shifts in a direction that tends to relieve the effect of an applied stress [120]. Thus, an increase H_3O^+ ions in the solution causes to shift the position of the equilibrium to the left side. i.e. the solubility of the salt will decrease. While, the addition of OH^- ions will have the opposite effect. *This may be accepted as an explanation for the change in the solubility of the solution after the change in the pH-value of the solution.*

The change in the structure of the solution by the presence of various ions can be estimated from the entropy data (order or disorder of the system) shown in **Table 6.3.1.** If the entropy of an electrolyte has a more negative value, then it is a structure

former. If the value is less negative, then it is a structure breaker. For this work the following can be summarised [121]:

- H_3O^+ is a slight structure breaker.
- Cations smaller or more highly charged than H_3O^+ are structure formers.
- OH^- is a structure breaker, while SO_4^{2-} is a structure former.

Table 6.3.1.: Physical properties of cations and anions at 298 K [122].

| <i>Physical properties</i> | | | | |
|----------------------------|----------------------------|--------------------------------------|---|--------------------------------------|
| Ion | <i>Ionic Radii</i> [Å°] | H_{hyd} [KJ.mol ⁻¹] | S_{hyd} [KJ.mol ⁻¹ .K ⁻¹] | G_{hyd} [KJ.mol ⁻¹] |
| H_3O^+ | — | -1129 | -131 | -1090 |
| Na^+ | 0.95 | -444 | -110 | -411 |
| K^+ | 1.33 | -360 | -74 | -338 |
| Fe^{+2} | 0.76 | -2305 | -383 | -2191 |
| Mg^{+2} | 0.65 | -1999 | -311 | -1906 |
| Ni^{+2} | 0.72 | -2490 | -396 | -2372 |
| Pb^{+2} | 1.2 | -1785 | -228 | -1717 |
| Cl^- | 1.81 | -340 | -76 | -340 |
| OH^- | 1.4 | -423 | -149 | -379 |
| SO_4^{2-} | 1.5 | -1145 | -263 | — |

In supersaturated solution, neutral solution, Mg^{+2} ions will move towards the crystal surface (the crystal growth will be enhanced), while in undersaturated solution Mg^{+2} ions will leave the crystal surface towards the solution (the dissolution rate will be enhanced). In the same way, the addition H_3O^+ ions to the solution (acidic medium) will make the solution unstable (structure breaker). Consequently, in supersaturated solution it is proposed that, the Mg^{+2} ions prefer to remain in the solution (as aqueous ions $Mg(OH)^+$ see Eq. 6.2). Therefore, the number of Mg^{+2} ions arriving to the crystal surface will be reduced, therefore, the growth rate will be

suppressed. In undersaturated solution the number of Mg^{+2} ions that must leave the crystal surface towards the solution will be reduced, therefore, the dissolution rate will be suppressed. *This may be accepted as an explanation for a lower growth and dissolution rate of $MgSO_4 \cdot 7H_2O$ crystals in acidic/alkaline solutions compared with the neutral solutions.*

6.3.2. The effect of K^+ ions ($MgSO_4 \cdot 7H_2O$ experiments)

It can also be seen from the thermodynamic properties of the ions shown in **Table 6.3.1.** The smaller the ion is, the stronger the interaction (higher hydration energy) between the ion and water molecules in the coordination sphere, that is to say univalent, divalent and trivalent positive ions (cations) are hydrated. The largest enthalpy of hydration can be expected for the smallest ion (e.g. Mg^{+2} has enthalpy $-1999 \text{ kJ mol}^{-1}$). Therefore, the presence of such an ion in the solution has more tendencies for interaction with water molecules than the largest ion, especially, when the latter has such a relatively small enthalpy of hydration (K^+ has enthalpy -360 kJ mol^{-1}). *It is proposed that such an interaction stands behind the increase in the solubility of $MgSO_4 \cdot 7H_2O$ in the presence of K^+ ions in the solution. The later inference has proven the results concerning the increase in the solubility of $MgSO_4 \cdot 7H_2O$ by adding K_2SO_4 and KH_2PO_4 as impurities (see **Table 5.2.1.**).*

As mentioned previously the change in the structure of the solution by the presence of various ions can be estimated from the entropy data (order or disorder of the system) shown in **Table 6.3.1.** Here the following can be summarised:

- K^+ is a slight structure breaker.
- A cation smaller or more highly charged than K^+ is a structure former.

Here it is proposed, that the presence of K^+ ions in the solution will make the solution unstable (structure breaker). Consequently, K^+ ions prefer to move toward the crystal surface rather than to remain in the solution (as aqueous ions). *Therefore, the number of K^+ ions adsorbing on the crystal surface will be increased by increasing the amount of K^+ ions adding to the solution, hence the number of Mg^{+2} ions arriving at the crystal surface will be reduced (the growth rate will be suppressed). This may be accepted as an explanation for suppressed growth rate compared to the pure solution.*

6.3.3. The effect of hydro-complex ions

6.3.3.1. $MgSO_4 \cdot 7H_2O$ experiments

In the Fe^{+2} ions-free solution the growth rate of $MgSO_4 \cdot 7H_2O$ crystals is affected by pH-value of the solution [109]. However, in the presence of Fe^{+2} ions the growth rate changed significantly with pH (the pH of Fe^{+2} ions contaminated solution decreased to a value of 4.32 and 3.46 corresponding to Fe^{+2} ions concentration of 1 and 2 wt %, respectively [108]). This decrease in pH is due to the hydrolysis reaction of the hydro-complex compound of Fe^{+2} ions [65, 119]. The impurity effect, $\alpha\theta_{eq}$, of Fe^{+2} ions decrease dramatically as the pH was increased (see *Fig. 6.3.1.*).

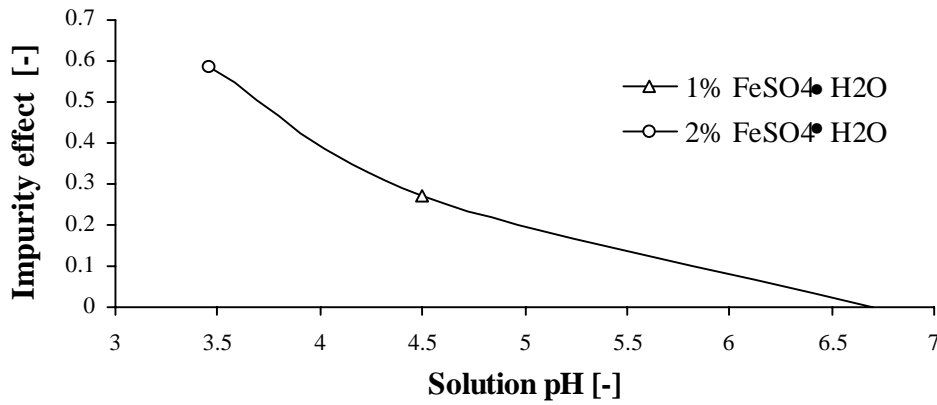


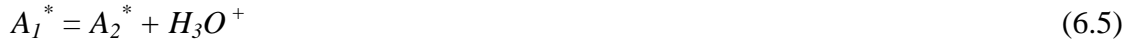
Figure 6.3.1.: Effect of the pH-value on the impurity effect, $\alpha\theta_{eq}$, at $\sigma = 0.01$.

This result suggests that only part of the adsorbed is growth suppression active. Fe^{+2} ions do not dissolve as bare ions in water but dissolve as hydro-complex ions, producing H_3O^+ ions through hydrolysis reaction like an acid [65, 119]:



Fe^{+2} ions may also dissolve in $MgSO_4 \cdot 7H_2O$ solution in the same way and the hydro-complex ion exchange water molecules with sulfate ions (ligand exchange reaction). The ligand exchange reaction products may also give dimers, which can be also hydrolysis products. The chemistry of Fe^{+2} in $MgSO_4 \cdot 7H_2O$ solution is complicated. For simplicity, only two hydrolysis reaction will be considered here,





where A is an inactive (both for growth-suppresses and adsorption) hydro-complex compound, A_1^* and A_2^* are hydrolysis products, which could be assumed to be $Fe(OH)^+$ and $Fe(OH)_2$, respectively. Further, it is assumed that these two hydrolysis products both adsorb on the surface of the crystal to be grown (adsorption active) but only A_1^* acts as a growth suppression active species. The concentration of the first hydrolysis product, $[A_1^*]$, (and hence the amount of adsorbed A_1^*) is speculated to decrease in the highr pH range, as discussed below. The concentration, $[A_1^*]$, depends on the relative values of quotients, Q_1 and Q_2 , the equilibrium constants defined with actual concentrations, $[A]$, $[A_1^*]$, $[A_2^*]$ and $[H_3O^+]$, by:

$$Q_1 = [A_1^*][H_3O^+]/[A], \quad (6.6)$$

$$Q_2 = [A_2^*][H_3O^+]/[A_1^*]. \quad (6.7)$$

As discussed in detail by Guzman et al. [123] in relation to the impurity effect of Cr^{+3} ions on crystal growth of K_2SO_4 the concentration of A_1^* can be written by Eq. 6.8 as a function of pH with the aid of a simple mass balance ($c_{imp}=[A] + [A_1^*] + [A_2^*]$) and Eqs. 6.6 and 6.7,

$$[A_1^*] = f_1(pH)c_{imp}, \quad (6.8)$$

where $f_1(pH)$ is a fraction of A_1^* present in the solution to the total impurity dissolved, which is a function of the pH:

$$f_1(pH) = \frac{\frac{Q_1}{[H_3O^+]}}{1 + \frac{Q_1}{[H_3O^+]} + \frac{Q_1Q_2}{[H_3O^+]^2}} = \frac{Q_1}{10^{-pH} + Q_1 + \frac{Q_1Q_2}{10^{-pH}}} \quad (6.9)$$

The function, $f_1(pH)$, and hence, $[A_1^*]$ decreased as the pH is increased in the range of $pH \geq -\log(Q_1Q_2)^{1/2}$ (see **Fig. 6.3.2.**). This could be a reason why the growth rate decreased contrary to the increasing trend of the adsorbed Fe^{+2} ions. The adsorption isotherm for the growth suppression active species, A_1^* , could be written as,

$$\theta_{eq1} = \frac{K[A_1^*]}{1 + K[A_1^*]} = \frac{Kf_1(pH)c_{imp}}{1 + Kf_1(pH)c_{imp}} \quad (6.10)$$

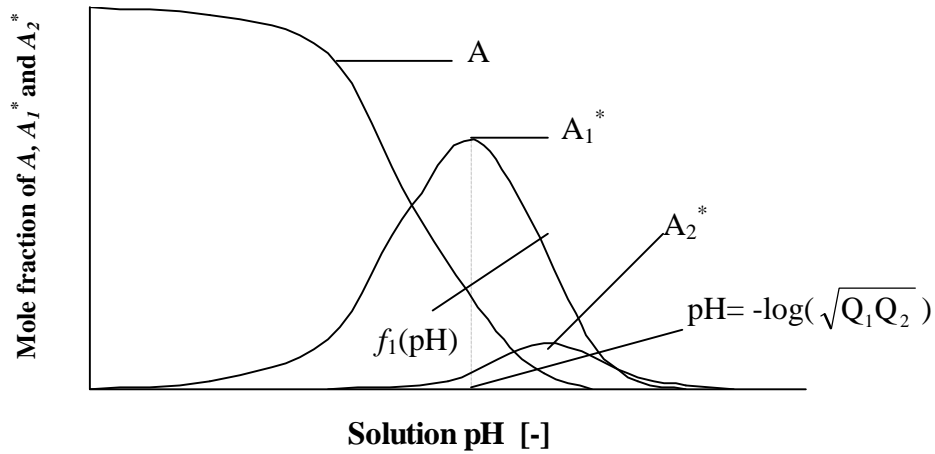


Figure 6.3.2.: A simple schematic representation of $[A]$, $[A_1^*]$ and $[A_2^*]$ as a function of pH [65].

Strictly speaking the effect of Fe^{+2} ion concentration on the growth kinetics in terms of surface coverage, θ_{eq} Eq. 3.36, should be considered by using Eq. 6.10. But it is impossible because θ_{eq1} is not determined experimentally. The larger the impurity effectiveness factor, α , is expected with respect to A_1^* (not the total dissolved impurity, c_{imp}), since $K > Kf_1(pH)$ and $\theta_{eq} > \theta_{eq1}$. The increasing trend of impurity effect, $\alpha\theta_{eq}$, with increasing impurity concentration is consistent with the increasing behaviour of θ_{eq} expected from the theory (see Eq. 6.10) under a constant impurity effectiveness factor, α , as shown in **Fig. 6.3.3.** The effect of pH on the growth behaviour is shown in **Fig. 6.3.4.**, the lower the pH, the stronger the impurity effect becomes. This pH effect can be explained as a result of increasing surface coverage, θ_{eq} , **Fig. 6.3.3.** and Eq. 6.10.

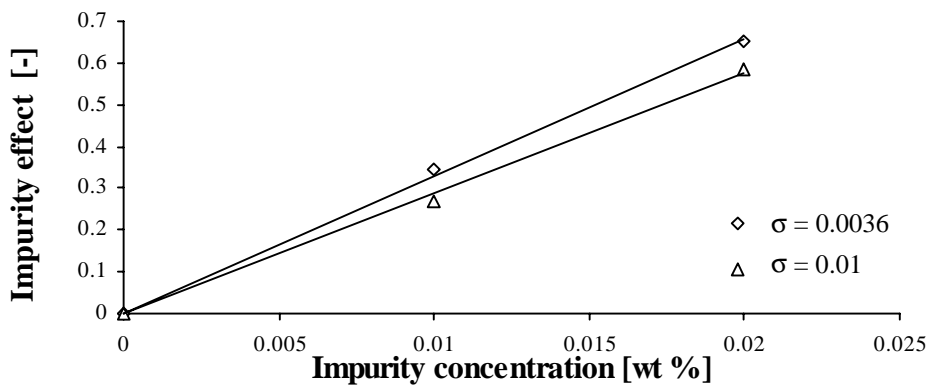


Figure 6.3.3.: Effect of $FeSO_4 \cdot H_2O$ concentration on the impurity effect, $\alpha\theta_{eq}$.

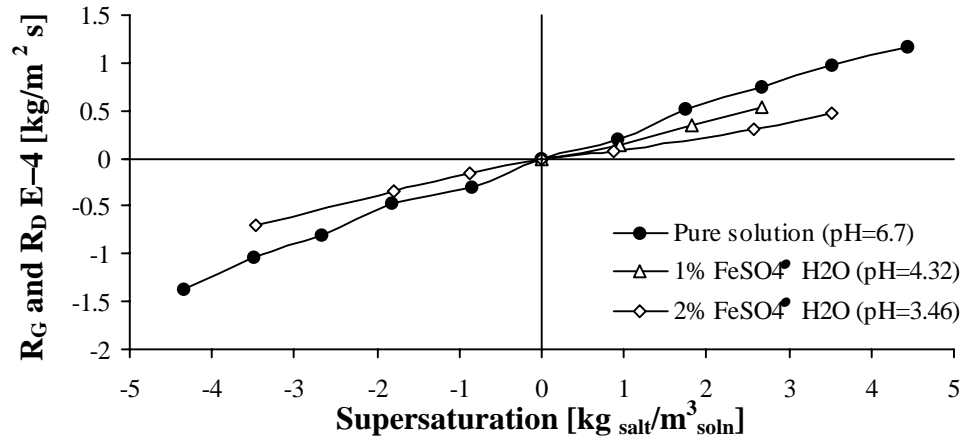


Figure 6.3.4.: Growth and dissolution rates of $MgSO_4 \cdot 7H_2O$ in the presence of $FeSO_4 \cdot H_2O$ as impurity.

The dissolution process is closely related to the growth process, since they are surface-related phenomena [4, 5]. In either process, Fe^{+2} ions have to be adsorbed or desorbed on/off the crystal surface. The dissolution is suppressed with increasing Fe^{+2} ions concentration in the solution as already shown in **Fig. 6.3.4.** The adsorption or desorption mechanisms of active Fe^{+2} ion complexes is expected to be the same during both the dissolution and the growth processes, i.e., if these complexes adsorb at growth layer steps and retard growth, it is reasonable to assume that they desorb at dissolution layer steps and retard dissolution. The need for much higher critical concentrations of Fe^{+2} ions for dissolution retardation than for growth retardation have not been satisfactorily explained, but the diffusional and kinetic processes involved are fundamentally different in the two cases. Dissolution, a much faster process is an exact reversal of growth. Solute ions are detached from the layer as a direct consequence of hydration and are transported directly, by volume diffusion, to the bulk solution. Impurity adsorption at layer fronts prevent dissolution (or disintegration with hydration), but they are readily removed during the dissolution process. Consequently, larger amounts of impurities are necessary to prevent water molecules reaching and reaction with the solute ions.

The same argument in the presence of Ni^{+2} ions, as impurity, can be applied for suppressing the growth and dissolution rates of $MgSO_4 \cdot 7H_2O$ crystals.

6.3.3.2. NaCl experiments

By addition of Na^+ ions to the water, the hydronium ions are generated as shown in the following expression:



The position of the equilibrium will be affected by adding Mg^{+2} ions to the saturated solution as impurity and the later, according to Eq. 6.1, it will cause to generate hydronium ions (H_3O^+). Thus, an increase H_3O^+ ions in the solution causes to shift the position of the equilibrium to the left side, principle of Le Chatelier [120], i.e. the solubility of the salt will decrease. *This may be accepted as an explanation for the change in the solubility of NaCl in the presence of Mg^{+2} ions in the solution.*

As mentioned previously, the largest enthalpy of hydration can be expected for the smallest ion (e.g. Mg^{+2} has enthalpy $-1999 \text{ kJ mol}^{-1}$, see **Table 6.3.1.**). Therefore, the presence of such an ion in the solution has more tendencies for interaction with water molecules than the largest ion, especially, when the latter has such a relatively small enthalpy of hydration (Na^+ has enthalpy -444 kJ mol^{-1}). *It is proposed that such an interaction stands behind the decrease in the solubility of NaCl in the presence of Mg^{+2} ions in the solution (see **Fig. 5.1.1.**).*

The presence of various ions in the solution cause to the change in the structure of the electrolyte solution. This change can be estimated from the entropy data presented in **Table 6.3.1.**. In this case the following can be summarised:

- Na^+ is a slight structure breaker.
- A cation smaller or more highly charged than Na^+ is a structure former.

In supersaturated solution, pure NaCl solution, the crystal growth will be enhanced by adsorption of Na^+ ions on the crystal surface, while in undersaturated solution, Na^+ ions will leave the crystal surface towards the solution (the dissolution rate will be enhanced). In the same way, the presence of Mg^{+2} ions in the solution will give the solution more stability (structure former). Consequently, in supersaturated solution it is proposed that, Mg^{+2} ions will be moved toward the crystal surface and adsorbed on the surface, while Na^+ ions prefer to remain in the solution (as aqueous

ions). Therefore, the number of Na^+ ions arriving at the crystal surface will be reduced, hence the growth rate will be suppressed.

This may be accepted as an explanation for suppressed growth rate compared to the pure solution. The same argument in the presence of Pb^{+2} ions, as impurity, can be applied for suppressing the growth rate of NaCl crystal.

In another conclusion, Mg^{+2} ions do not dissociate as bare ions in water but they dissociate as hydro-complex ions, producing H_3O^+ through hydrolysis reaction as shown in Eq. 6.1. Mg^{+2} may also dissociate in $NaCl$ solution in the same way and the hydro-complex ion exchange water molecules with chloride ions (ligand exchange reaction). The ligand exchange reaction products may also give dimers, which can also be hydrolysed. The chemistry of Mg^{+2} in $NaCl$ solution is complicated. For simplicity, only two hydrolysis reactions will be considered (see Eqs. 6.6 and 6.7), where A , is assumed to be Mg^{+2} , is an inactive (both for growth-suppresses and adsorption) hydro-complex compound, A_1^* and A_2^* are hydrolysis products, which could be assumed to be $Mg(OH)^+$ and $Mg(OH)_2$, respectively. Further, it is assumed that these two hydrolysis products both adsorb on the surface of the crystal to be grown (adsorption active), but only A_1^* acts as a growth suppressing active species. The concentration of the first hydrolysis product, $[A_1^*]$, (and hence the amount of adsorbed A_1^*) is speculated to decrease as discussed, previously, in relation to the impurity effect of Fe^{+2} ions on crystal growth of $MgSO_4 \cdot 7H_2O$ [108].

6.4. Electrical double layer

At the interface of a charged solid and a liquid there is always a separation of electrical charge. The surface of the solid has an excess of one charge and the balancing is found in the adjacent surface region of the liquid. The arrangement of the charges at the solid and liquid interface is referred to as the double layer.

The double layer is an electrical cloud near the solid surface composed of both a rigid zone, known as the Stern layer and a diffuse layer. Ions having the opposite charge as the solid are immediately attracted to the surface of the solid and attach, forming the Stern layer. Additional ions of the same charge as the Stern layer are also attracted by the oppositely charged solid's surface but are simultaneously repelled by the like charges in the Stern layer. This dynamic equilibrium results in the formation of a diffuse layer. The diffuse layer is also composed of ions with the same sign of charge as the solid with the concentration of these ions decreasing with distance from the solid. Together the Stern layer and the diffuse layer form the double layer (*Fig. 3.4.3.*). The thickness of the double layer is a function of the pH and ionic strength of the solution. The boundary between the Stern layer and the diffuse layer is called the shear plane. The electric potential at the shear plane is called the zeta potential. A change in zeta potential reflects a change in surface charge.

6.4.1. Charged particles

The lattice ion hydration theory describes surface charge development by nonreactive ionic solids when placed in water. This theory applies to ionic solids that do not undergo surface oxidation reactions. Either reaction type would modulate the surface charge that the solid develops in water. The only reaction of consequence then is the hydration of lattice ions, and the differential hydration of these lattice ions at the surface of the solid determines the sign of the surface charge.

The theory as first proposed by de Bruyn and Agar [124] was for simple uni-univalent salts in which the cation and anion are in interchangeable lattice positions, which is to say that their lattice energies are equivalent. In this elementary case, the surface charge can be estimated simply from a comparison of the hydration free energies of the corresponding gaseous ions. The theory was demonstrated for the silver halides [124]. Recently, the lattice ion hydration theory was extended to take

into consideration lattice energies effects which were shown to be particularly significant for more complicated nonreactive ionic solids such as calcium fluoride [125]. Thus, a more complete theoretical treatment considers the lattice energy of surface ions which in turn are dependent on the crystal structure and preferential plane of cleavage. The energetic can be represented, for the solid MX , as follows:



If the hydration energy of the surface lattice cation is more negative than the hydration energies of the surface lattice anion, as described by reaction 3 (Eq. 6.14), then the surface of MX will carry a negative charge. The converse is also true. The complete analysis requires knowledge of the hydration free energies for gaseous ions (reaction 1 (Eq. 6.12)) and the lattice energy for surface ions (reaction 2 (Eq. 6.13)). The former is available from the literature as determined from the Born and Mayer theory [126], while the latter is determined from electrostatic principles, taking into consideration the geometric arrangement of cations and anions in the lattice as described by the surface Madelung constant [125].

As discussed previously in **Chapter 6.3.** and as shown in **Table 6.3.1.** that the largest energy, enthalpy and entropy of hydration can be expected for the smallest ion (e.g. Mg^{+2} ion) compared to SO_4^{-2} ion [121]. *Therefore, here it is proposed that Mg^{+2} ions have more energy of hydration than SO_4^{-2} ion. Consequently, according to the above theory it may be concluded that the surface of a $MgSO_4 \cdot 7H_2O$ crystal is carrying a negative charge.*

6.4.2. Measuring crystal charge (ζ -potential)

The charge impacted to crystals dispersed in water is called ζ -potential. Instruments designed to measure the value of ζ -potential do so by subjecting the sample to an electric field and then observing the movement of crystals toward an

electrode of an electrophoresis cell. The sign of the charge of the crystals in the electric field determines direction of movement. A negative charge on the crystals causes it to move toward a positive electrode. A positive charge on the crystal would cause it to move toward the negative electrode. The velocity of the crystal movement is determined by the amount of charge. The velocity of movement of the crystals is measured by evaluating the Doppler shift of scattered light. The velocity of crystal movement is directly related to its charge. The ζ -potential is calculated from the velocity. ζ -potential is expressed in millivolts (mV). Here, it is important to note that the surface potential is actually of the opposite sign of the perceived potential, due to the adsorbed ions performing a charge reversal [100].

In general, $MgSO_4 \cdot 7H_2O$ crystals suspended in a saturated solution have a positive ζ -potential at different electric field applied as shown in **Fig. 6.4.2.** I.e. the $MgSO_4 \cdot 7H_2O$ crystals are negatively charged. The later inference proves the validate of the above conclusion (**Chapter 6.4.1**), that the surface of $MgSO_4 \cdot 7H_2O$ crystals carry a negative charge from the standpoint of the lattice ion hydration theory.

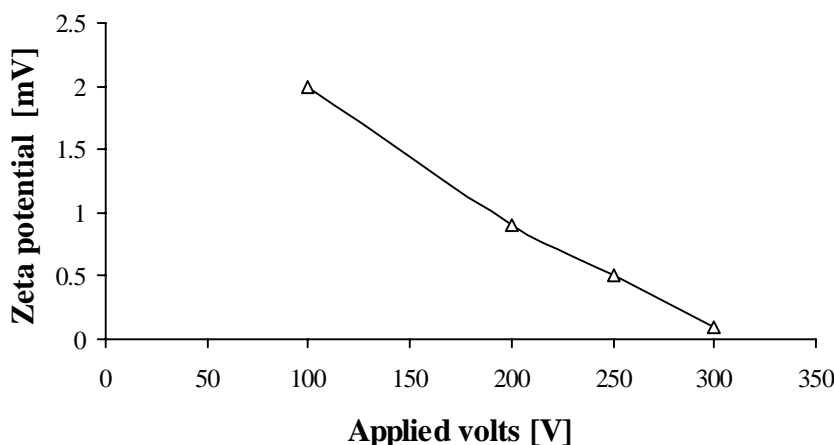


Figure 6.4.2.: Zeta potential measurements for $MgSO_4 \cdot 7H_2O$ crystals at different applied electric field.

Fig. 6.4.3. shows the mobility and the conductivity of the ions at differently applied electric fields. It is clear from **Fig. 6.4.3.** that by increasing the applied of electric field the mobility of the ion will be decreased, while the conductivity of the ions tend to increase. According to Eqs. 3.47 and 3.48, it is true that the mobility of the ions tend to decrease with increasing the electric field and hence the ζ -potential of the diffusion layer will be decreased. In another conclusion the conductivity of the

double layer, λ_c , depends linearly on the mobility, u , and the concentration, c , of the ions and may be expressed by the following equation from the theory of electrolytes [127]:

$$\lambda_c = c_+ u_+ e z_+ + c_- u_- e z_- \quad (6.15)$$

The mobility of the ions depends on the activation energy of migration, E_{mig} , which irrespective of their charge can be expressed as follows [127]:

$$u = u_0 \exp(-E_{mig}/k_B T) \quad (6.16)$$

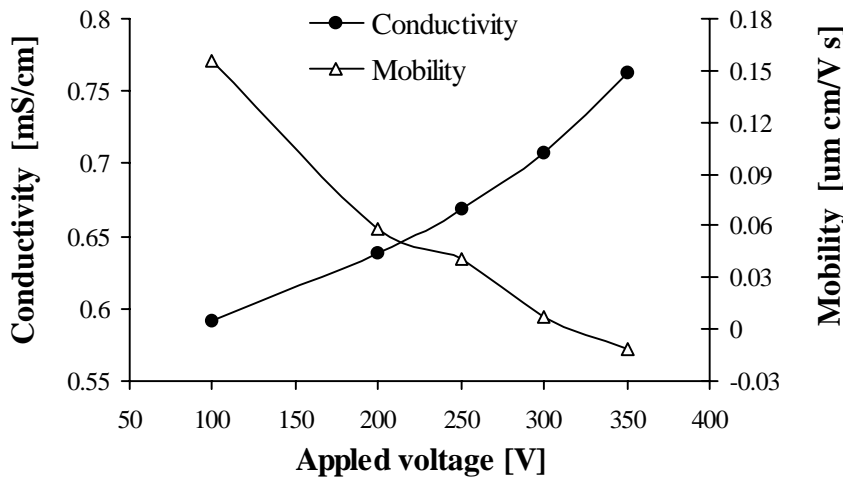


Figure 6.4.3.: Electrophoretic mobility and conductivity of Mg^{+2}/SO_4^{-2} ions at different electric field.

The thickness of the diffusion layer will be bigger by the decreasing potential near the crystal surface relative to the bulk of the solution (see Eq. 3.58). This broad of the thickness of the diffusion layer will slow down the diffusion step of the crystallization kinetics, i.e. the movement of Mg^{+2}/SO_4^{-2} ions inside the diffusion layer will be decreased. The conductivity is increased by increasing the electric field and according to Eq. 6.15 this may be attributed to the increasing of the ionic strength inside the diffusion layer. The present results already indicate that the surface charge of particles are described by measurements of their electrophoretic mobility and the calculation of the corresponding ζ . The potential in the region of shear some distance away from the crystal surface. The measured ζ then provides information regarding

the sign (positive/negative) of the prevailing charge at the crystal's surface. Crystals in aqueous electrolyte acquire a charge due to chemical dissociation of the surface groups. This causes the formation of the electrical double layer. Any ion, which will be incorporated in the crystal lattice, should pass through this electrical double layer, which gives extra resistance to crystal growth. If the formation of the electrical double layer is accepted, external effects on this layer and on the crystallization kinetics can be explained more easily.

6.4.3. Effect of pH

Any metal ion in solution is in "equilibrium" with a variety of species e.g., hydrolysis species in aqueous solution that originate from dissolution of the metal ions (see Eq. 6.1). Such hydrolysis species adsorb preferentially and the adsorption of complex hydrolysis ions is responsible for the surface properties of metal hydroxyl. Any ion with a nonelectrostatic adsorption energy contribution can be regarded as preferentially or specifically adsorbed. Within this broad grouping a further division can be made between those ions that adsorb chemically (sharing of electrons) and those do not. For chemical interaction an ion must penetrate the Stern layer. A chemical interaction with the surface is experimentally evidenced by superequivalent adsorption, by reversal of the ζ -potential, or by a shift in the *point of zero charge* (*pzc*). In the absence of specific adsorption the *pzc* is identical. The direction of shift is indicative of the sign of the charge on the ion that is specifically adsorbing. The metal hydroxyl surface, which has a positive ζ -potential, responds by becoming more positive as the pH is lowered. If the pH is raised it becomes more negative. The surface therefore tends to be more negative the higher the pH and more positive the lower the pH gets. At some intermediate pH these ions, i.e. H_3O^+ and OH^- , which are responsible for generating the surface charge are called the potential determining ions for the system.

As mentioned previously $MgSO_4 \cdot 7H_2O$ crystals suspended in a saturated solution have a positive ζ -potential charge. By adding more acid to this suspension makes the crystals tend to acquire more positive charges. Adding alkali to the suspension leads to the point where the charge will be neutralized. Further addition of alkali will cause a build up of a negative charge as shown in **Fig. 6.4.4.** According to

Eq. 3.45 the potential of the double layer is increased at low pH values and decreased (to a negative charge value) at high pH values.

As a result, according to Eq. 3.58, the highest potential will be at the surface and will be decreased gradually with distance from the surface. The increase of the potential difference as a result of charging the crystal surface will affect the thickness of the diffusion layer. The thickness of the diffusion layer will be smaller by the increasing potential near the crystal surface relative to the bulk of the solution. This reduction of the thickness of the diffusion layer will accelerate the diffusion step of the crystallization kinetics, i.e. the movement of Mg^{+2}/SO_4^{-2} ions inside the diffusion layer will be accelerated. On the other hand, the adsorption of H_3O^+/OH^- ions on the crystal surface will prevent the adsorption of Mg^{+2}/SO_4^{-2} ions even though the later have a higher velocity than the ions in the bulk. *This is one reason behind the experimentally observed suppression of the growth rate of $MgSO_4 \cdot 7H_2O$ crystals as presented in Fig. 5.2.4.*

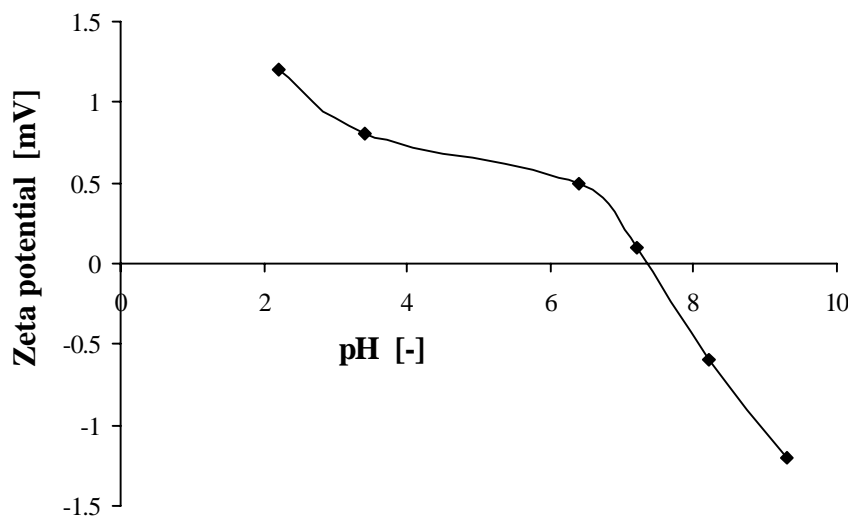


Figure 6.4.4.: *Experimental measurements of zeta potential versus pH values at an applied electric field 250 V.*

On the another side, increasing the potential of the double layer, to more positive charges, by increasing the adsorption of H_3O^+ ions increases the conductivity of the double layer as experimentally observed in **Fig. 6.4.5.** This mean that the mobility of the ions will be increased. In another words, according to Eq. 6.16, the activation energy of migration of the ions within the double layer will be reduced by the adsorption of H_3O^+ ions at the crystal surface and hence the growth rate will be

decreased. By adsorbing OH^- according to Eq.6.16 the activation energy, E_{mig} , of the ions will be increased. This increases do not effect the conductivity of the double layer, on the contrary the adsorption of H_3O^+ ions. The later inference may be attributed to the reversing the sign of the surface charge to a negative charge. It may be concluded that the conductivity of the ionic strength has a significant effect but not sufficient as an explanation for the crystallization processes. Therefore, taking the adsorption of H_3O^+ / OH^- ions on the crystal surface and their effect on the surface potential and surface charge prove to be important in crystallization phenomena.

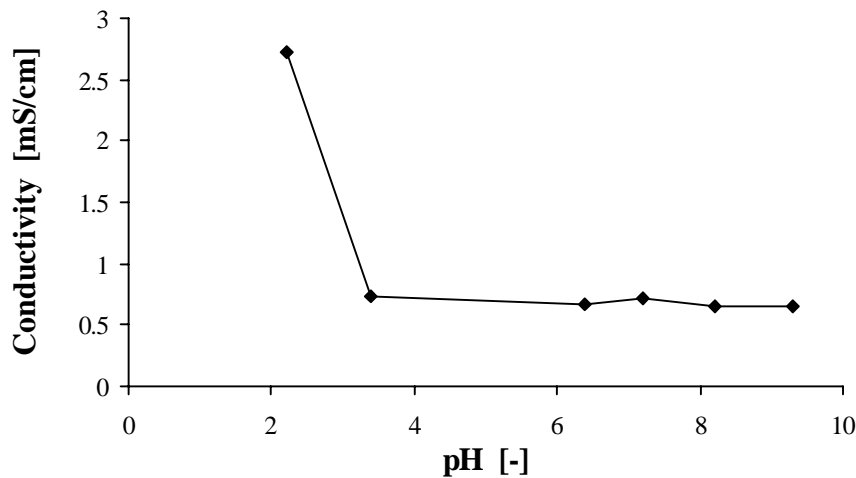


Figure 6.4.5.: Conductivity of $MgSO_4 \cdot 7H_2O$ crystals versus pH values at an applied electric field 250 V.

Taking the change in the structure of the solution into account gives a good agreement of found results and understandings of physical phenomena but is still not enough as an explanation for the total crystal growth phenomenon. Especially, in the case of the effect of the adsorption of H_3O^+ / OH^- ions on the potential and charge of the diffuse layer was not be considered so far. It is proven that, the results of ζ measurements indicate that pH plays an exceptional role at the $MgSO_4 \cdot 7H_2O$ crystals surface as shown by the following observation:

- H_3O^+ ions cause ζ to become more positive than neutral solution.
- OH^- ions change the sign of ζ to more negative than neutral solution.

6.4.4. Effect of adsorption ions

Effect of the increasing ionic strength on the ζ -potential of the lattices may shield the charge of the ionic groups on the surface, change in distribution of the counter-ions and the co-ions in the electric double layer and a decrease in thickness of the electric double layer adjacent to the surface. It is normally accepted in colloidal systems that the charge reversal phenomena occur at higher concentration of inorganic electrolyte when the polarization energy of counter-ions for the interaction with the fixed charge species is sufficiently high. Thus, the total potential across the double layer, commonly referred to as the surface potential, Ψ_0 , is determined only by the concentration of potential-determining ions in solution. Indifferent electrolytes do not affect its value unless they have a secondary effects. The ζ -potential is more complex and affected by all electrolytes, the effect depending not only on concentration but also on the valence and sign of charge of the ions. Increasing the concentration of indifferent electrolytes in solution reduces the value of ζ -potential by compression of the double layer because more ions are forced into Stern layer.

To ascertain the effect of ionic strength on the ζ of $MgSO_4 \cdot 7H_2O$ when the crystal surface is positively or negatively charged, ζ was measured as a function of the concentration of different impurities. As shown in **Table 5.2.1.** the growth rate of $MgSO_4 \cdot 7H_2O$ crystal was suppressed by adding impurities and the suppressing of growth rate is more pronounced at higher impurities concentration except in the presence of $MgCl_2$ as impurity, in this case, it was no noticeable effect on the growth kinetic of $MgSO_4 \cdot 7H_2O$ crystals. To confirm this idea, the effect of adding different impurities on the ζ of $MgSO_4 \cdot 7H_2O$ crystals was investigated.

Fig. 6.4.6. shows the effect of impurities concentration of K_2SO_4 , KH_2PO_4 , KCl , Na_2SO_4 and $MgCl_2$ on the value of ζ of $MgSO_4 \cdot 7H_2O$ crystals. The experiments show that K_2SO_4 and KH_2PO_4 exert an identical influence on ζ of $MgSO_4 \cdot 7H_2O$ crystals over the entire concentration range investigated. The reversal of ζ sign occurs by adding KCl and Na_2SO_4 to the solution. It is clear that the effect of K^+ , Na^+ and $H_2PO_4^-$ ions on ζ indicates that these ions play a special role at the $MgSO_4 \cdot 7H_2O$ crystals surface.

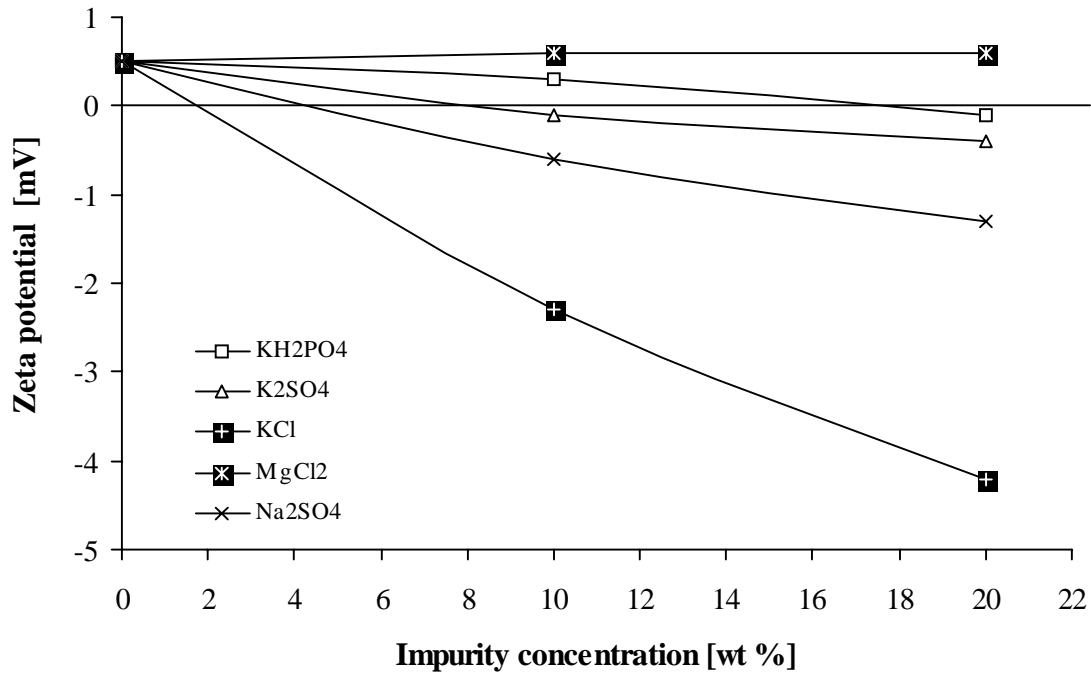


Figure 6.4.6.: The effect of different impurities concentrations on the ζ -potential of $MgSO_4 \cdot 7H_2O$ crystals.

In this study, two main types of ions are considered:

1.. Potential-determining ions

Mg^{+2} and SO_4^{-2} ions are potential-determining ions for $MgSO_4 \cdot 7H_2O$ surface. Since, adsorption of SO_4^{-2} ions on the surface of $MgSO_4 \cdot 7H_2O$ will reduce the value of ζ . This is attributed to the negative charge of SO_4^{-2} ions which will cancel some of the positive charges on the $MgSO_4 \cdot 7H_2O$ crystals. While, in the case of adsorption of Mg^{+2} ions on the surface causes an increase in the value of ζ . Observations in **Fig. 6.4.6.** show that the adsorption of Mg^{+2} ions have a relatively weak effect on the value of ζ . *The later inference is accepted as an explanation for the no noticeable kinetic effect on the growth rate of $MgSO_4 \cdot 7H_2O$ crystals in the presence of $MgCl_2$ impurity (see Table 5.2.1).*

2.. Indifferent ions

Which are subdivided into *surface-active* and *surface-inactive* indifferent ions. Each of these types of ions can be characterized by its effect on the *zeta potential*.

1. surface-inactive indifferent ions

Surface-inactive electrolytes reduce the value of ζ by compression of the double layer without changing its sign. ζ approaches zero as a limiting value at higher concentration.

2. surface-active indifferent ions

If the counter-ions are attracted to the surface not only by simple electrostatic forces, but also by strong chemical or covalent forces, they may reverse the sign of ζ as in the presence of K^+ , Na^+ and Ni^{+2} ions (see **Figs. 6.4.6.** and **6.4.7.**). When potential-determining ions, such as OH^- ions change the sign of ζ , the charge at the surface as well as Ψ_0 must change sign; whereas, when a surface active counter-ion changes the sign of ζ , there must be a higher charge in the Stern plane than at the surface. This results in the formation of a *Triple-layer* [128].

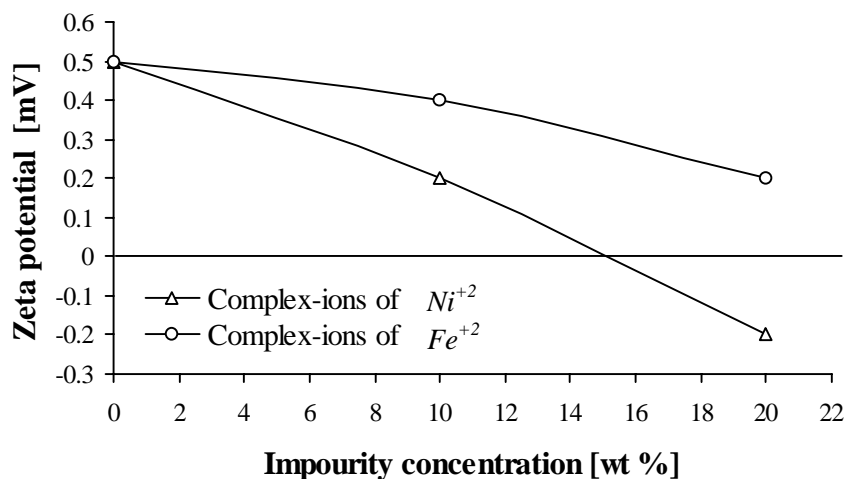


Figure 6.4.7.: The effect of hydro-complex ions of Ni^{+2} and Fe^{+2} on the ζ -potential of $MgSO_4 \cdot 7H_2O$ crystals.

The Triple-layer model suggested that, the solid-liquid interface visualized in terms of three layers of charge [128]:

1st layer: innermost layer, the surface layer consists of the solid surface itself; locale of *primary potential-determining ions* (e.g. Mg^{+2} , H^+ , SO_4^{-2} and OH^-).

- 2nd layer:** the *inner Helmholtz plane (IHP)*, a *compact-layer* of counter-charge typically consisting of relatively strong bounded (i.e. *specifically adsorbed*) ions (e.g. K^+ , Na^+ , Ni^{+2} and $H_2PO_4^-$).
- 3rd layer:** the *diffuse-layer* the location of ions termed *indifferent ions*. Ions only weakly attracted to the solid surface. The plane of the *diffuse-layer* closest to the solid surface is designated the *outer Helmholtz plane (OHP)*.

If K^+ , Na^+ and Ni^{+2} were *specifically adsorption ions*, ζ would have become more negative on increasing the concentration of impurities, and this has been observed experimentally as shown in **Figs. 6.4.6.** and **6.4.7.**

The decrease of ζ as a result of charging the crystal surface will affect the thickness of the *diffuse-layer*. The thickness of the *diffuse-layer* is relatively greater than the *compact-layer* by the decreasing potential near the crystal surface relative to the bulk of the solution. This broad of the thickness of the *diffuse-layer* will slow down the diffusion step of the crystallization kinetics, i.e. the movement of Mg^{+2}/SO_4^{-2} ions inside the *diffuse-layer* will be decreased. On the other hand, the thickness of *compact-layer* will be smaller comparison with *diffuse-layer*, this decreasing of the *compact-layer* thickness will accelerate the diffusion step. The *specifically adsorption ions* (e.g. K^+ , Na^+ and Ni^{+2}) were presented inside the *compact-layer* as suggested by the *Triple-layer* model. The presence such as ions causing a relatively strong bound on the crystal surface of $MgSO_4 \bullet 7H_2O$, thus the adsorption of Mg^{+2}/SO_4^{-2} ions is reduced. *This is one reason behind the experimentally observed suppression of the growth rate of $MgSO_4 \bullet 7H_2O$ crystals as presented in Table 5.2.1.*

Figs. 6.4.8. and **Fig. 6.4.9.** show the effect of different impurity concentration on the mobility and conductivity of ions, respectively. It is clear that by reducing the value of ζ by increasing the adsorption of *indifferent ions* increases the conductivity of the *double-layer* as experimentally observed in **Fig. 6.4.9.** While, the mobility of the ions is decreased. I.e., according to Eq. 6.16, the activation energy of migration of the ions within the double layer will be increased by the adsorption of *indifferent ions* at the crystal surface of $MgSO_4 \bullet 7H_2O$ and hence the growth rate will be decreased.

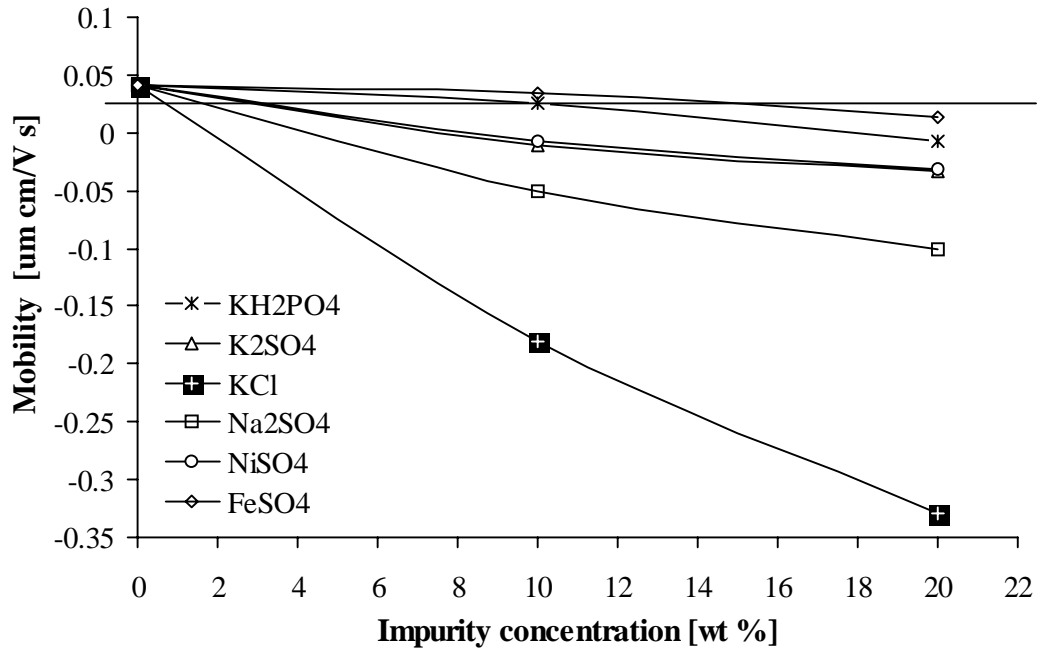


Figure 6.4.8.: Mobility of the ions as a function of different impurities concentration at an applied electric field 250 V.

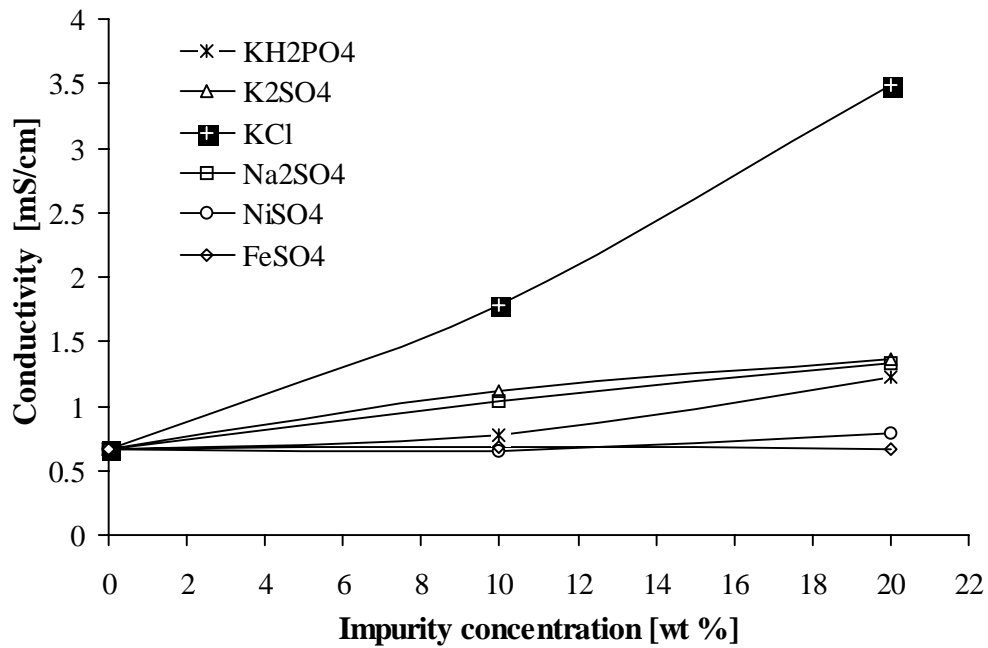


Figure 6.4.9.: Conductivity of the ions as a function of different impurities concentration at an applied electric field 250 V.

It is believed that, the Ni^{+2} ions are likely to interact with water molecules to form a complex ions in an aqueous solution (see Eq. 6.1). The ζ -potential charge changed from positive to negative when $NiSO_4$ was added. This result suggests that adsorption of the complex ions onto the crystal surface is possible. When a $Ni(OH)^+$ and $Ni(OH)_2$ ion adsorption occurs on the $MgSO_4 \cdot 7H_2O$ surface the Ni^{+2} charge on the surface of the $MgSO_4 \cdot 7H_2O$ is neutralized thus reducing the surface charge. Therefore, the decrease of ζ of $MgSO_4 \cdot 7H_2O$ can result from the adsorption of the complex ions, which replaces the adsorbed Mg^{+2}/SO_4^{-2} and reverses the positive value of ζ of the $MgSO_4 \cdot 7H_2O$ crystals. In an aqueous solution containing Ni^{+2} ions, complex ions are adsorbed onto the surface of the $MgSO_4 \cdot 7H_2O$ crystals and changed the polarity of the $MgSO_4 \cdot 7H_2O$ from positive to negative. This phenomenon was found in the suspensions containing $NiSO_4$ as electrolytes.

The same argument can be applied in presence of Fe^{+2} ions in the solution, as mentioned previously by adding Fe^{+2} ions to the saturated solution of $MgSO_4 \cdot 7H_2O$ the pH value of the solution is changed to a lower pH (see **Table 5.2.1.**). This decrease in pH is due to hydrolysis reaction of the hydro-complex compound of Fe^{+2} ions [65, 119]. An observation of **Fig. 6.4.7.** shows that the value of ζ is reduced by increasing Fe^{+2} ion concentration in the solution. This change in the value of ζ can be attributed by adsorption of H^+ and hydro-complex of Fe^{+2} ions on the crystal surface of $MgSO_4 \cdot 7H_2O$. If the change is attributed only by adsorption of H^+ ions, which are considered as *potential-determining ions*, this causes the ζ to become more positive as proven previously (see **Sec. 6.4.3** and **Fig. 6.4.4.**). If the case is attributed only for adsorption of hydro-complex of Fe^{+2} ions this causes to reverse the sign of ζ as in the case of the adsorption of hydro-complex of Ni^{+2} ions. Therefore, the reduction in the value of ζ in the presence of Fe^{+2} ions in the solution is reasonable to the adsorption of hydro-complex of Fe^{+2} and H^+ ions on the crystal surface of $MgSO_4 \cdot 7H_2O$ and hence this is causing a suppressing in crystal growth. Thus, the adsorption of H^+ ions on the crystal surface will cancel some of the negative charge of ζ that reasonable by adsorption of hydro-complex of Fe^{+2} ions.

6.5. Summary of results

From the results presented in this work the following conclusions may be drawn:

1. The influence of the heat transfer on the crystal growth kinetics in solution crystallization was often ignored. By the application of the Three-Step-model it is possible to quantify the importance of heat transfer on the growth kinetics. Especially for substances of high values for the crystallization heat or strong temperature dependencies of the equilibrium concentration this model leads to new predictions of the growth kinetics.
2. By taking the effectiveness factor concept into account good agreements are given for an explanation for the change in the controlling crystal growth mechanism in case of the growth of $NaCl$ and $MgSO_4 \cdot 7H_2O$ crystals in the presence of different impurities.
3. The proposed model (Eq. 3.39) can be used to show that the general relationship of crystallization kinetics in the presence of impurities is valid not only in the case of single crystals but also in industrial crystallizers where many crystals are growing in suspension. Consequently, from the analysis of the growth kinetics of different crystals it may be noted that the data are in general consistent with the proposed model (Eq. 3.39), and hence, the values of heat of adsorption, Q_{diff} , are to be considered sufficiently to determine whether adsorption occurs at kink sites or at the surface terraces. This is a valuable tool of knowledge in predicting growth phenomena.
4. The structure of the solution has been quite often ignored in the studies of crystallization kinetics of soluble salts. Taking the structure of the solution into account proves to be important in order to explain crystallization processes. Here, it is proven from previous conclusion that (see Chapter 6.3.3.) the growth behaviour is reasonably explained by a mechanism in which the hydrolysis product (hydro-complex compound of Fe^{+2} and Ni^{+2} ion) which is in equilibrium with the inactive hydrated complex in the solution, is assumed to be adsorbed on the growth layer steps of $MgSO_4 \cdot 7H_2O$ crystals and retards the growth. These trends in which the first

hydrolysis product of the hydro-complex compound of Mg^{+2} and Pb^{+2} acts as active species for growth inhibition of $NaCl$ crystals were the same as those of the hydro-complex compound of Fe^{+2} and Ni^{+2} ion.

5. The Laser-Doppler electrophoresis (ζ -potential measurements) was used to determine the electrophoretic mobility of $MgSO_4 \cdot 7H_2O$ crystals and thus predict the sign of surface charge in a saturated solution. Such information is of technological importance in the field of crystallization. It is evident from previous experimental results, that surface charge analysis of soluble salt systems is now possible using this Laser-Doppler electrophoresis after reducing the higher conductivity of saturated solution by diluting the solution with Ethanol. Further, by means of ζ -potential techniques it has been proven that $MgSO_4 \cdot 7H_2O$ crystals are positively ζ charged in pure solution. This charge is changed by presenting of potential-determining ions or indifferent-ions. The results of ζ measurements indicates that pH and cations/anions have a very strong effect on the electrical double layer. Consequently, they have a specific effect on crystallization, depending on how the surface charge is affected in way of increasing/decreasing or reversing the sign of the charge. Therefore, knowing the surface potential by measuring the ζ -potential can help to explain the crystallization phenomena which are not clear up to now.